Hindawi
Advances in Mathematical Physics
Volume 2023, Article ID 4349646, 10 pages
https://doi.org/10.1155/2023/4349646

Research Article

Quasilinear Hyperbolic Systems Applied to Describe the Magnetohydrodynamic Nanofluid Flow

Dayong Nie

Yellow River Conservancy Technical Institute, Kaifeng, China

Correspondence should be addressed to Dayong Nie; niedayong@yahoo.com

Received 20 October 2022; Revised 6 January 2023; Accepted 13 January 2023; Published 13 February 2023

Academic Editor: Ping Li

This study examines the flow of hyperbolic nanofluid over a stretching sheet in three dimensions. The influence of velocity slip on the flow and heat transfer properties of a hyperbolic nanofluid has been investigated. The partial differential equations for nanoparticle solid concentration, energy, and motion were turned into ordinary differential equations. Nanoparticle mass fluxes at boundaries are assumed to be zero, unlike surface concentrations. The influence of the main parameters on flow characteristics, surface friction coefficients, and the Nusselt number has been visualized. The results suggest that Brownian motion has a negligible impact on the heat transfer rate. The ratio of the elastic force to the viscosity force was found to decrease the fluid velocity. The resulting thermophysical properties of nanofluids are in agreement with previous research. The present findings can be used to expand the potential for using nanofluids as a coolant in critical thermophysical and industrial installations.

1. Introduction

Given the variety of scientific and technological contexts, more studies are needed to investigate how a viscous, incompressible nanofluid flows around a tensile plate. Some applications include solar receivers, polymer and plastic processing, and a variety of other industries. The effect of viscosity is especially noticeable near solid surfaces. According to the studies, the boundary layer thickness rises when the fluid's free motion exceeds the tensile speed. Furthermore, when working with fluid flows at the boundary of a solid, the friction force cannot be ignored.

Magnetohydrodynamics (MHD) has many uses. For instance, it can be applied in plasma research, and engineers turn to MHD when designing heat pumps, cooling reactors, flow metres, and generators. The authors in [1] investigated the flow of MHD micropolar nanofluids over nonlinearly stretched surfaces. When studying these kinds of flows, scholars looked at the effects of viscous dissipation, mixed convection, convective boundary conditions, and Joule heating. Other scholars explored the important role that friction between liquid and solid surfaces plays in mechanical devices [2]. Simultaneously, velocity slippage is an important factor to consider when assessing the physical properties of fluid flows in boundary layers.

Heat transfer and fluid flow characteristics of nonstationary, non-Newtonian fluids were modelled mathematically in [3]. The said article investigated how velocity slip, fluid buoyancy, and the Soret and Dufour effects affected nanofluid properties. These researchers discovered that decreasing the magnetic field while increasing the fluid sliding parameters increased fluid velocity.

A study of velocity slip conditions suggests that they only apply to macroscale systems [4]. Some researchers examined the effect of fluid slip in a dynamic context [5] and used the Bernstein collocation method to find a solution. Scholars also explored different slip regimes and how they affect the flow of boundary layers over nonlinearly compressible sheets [6]. For that, the dual solutions of fluid flow equations were found.

Some researchers explored the effect of a nonlinearly stretching sheet on the MHD mixed convection flow of a micropolar fluid [7]. Another study reported the results from a large-scale assessment investigating the MHD

boundary layer flow along a stretchable cylinder [8]. The authors focused on analyzing the thermal properties of fluid flow in axisymmetric boundary layers, as well as the velocity slip effects in homogeneous magnetic fields.

Another concern was the factors affecting the heat transfer properties of MHD (SWCNT-MWCNT) hybrid nanofluid flow in the presence of radiation [9]. A convectively heated disc stretched in the radial direction was reported to be the driving force behind the stationary critical flow of an electrically conductive fluid [10]. The investigation involved viscous dissipation and Joule heating effects, while the mathematical modelling was based on Jeffrey's defining fluid ratios.

Other effects on the boundary layer fluid flow were also studied, such as Brownian diffusion, thermal radiation, variable viscosity, magnetic field, and thermophoresis [11]. Furthermore, the heat and mass transfer characteristics of electrically conductive nanofluids were examined using radially extended convectively heated surfaces. The rate of stretching was assumed to be proportional to the radial distance. Some study investigated the transfer of radiative energy in a viscoelastic nanofluid while accounting for buoyancy forces and convection conditions [12]. The authors formulated a two-dimensional viscoelastic nanofluid flow using a rheological model that included thermophoretic and Brownian diffusions.

Many studies seek to comprehend the mechanisms that would substantially increase the heat transfer rates in nanofluids [13]. Particle migration, particle Brownian motion, and thermophoresis are some fundamental mechanisms that have been discussed in the literature [14]. Particle migration and thermophoresis are the most important mechanisms increasing the thermal conductivity of nanofluids, according to precious research [15]. Many investigations concerning the heat transfer of nanofluids utilize a Buongiorno model, such as in [16].

The thermal conductivity of conventional fluids is severely limited as well. The use of nanofluids with metal nanoparticles in suspension has recently become more common [17]. More studies emerged that explore the efficiency of nanofluids created by suspending nanoparticles in common fluids like paraffin oil, water, motor oil, or ethylene glycol [18]. In this case, nanoparticles act as agents to increase heat transfer rates while improving the thermal properties of the base fluids likewise [19].

Significant research efforts have been made to assess the degree of heat transfer intensification in nanofluids. These studies, for instance, included tests with various nanoparticle concentrations, base fluid selections, and particle sizes [20]. It has been established that the shape of nanoparticles influences the properties of nanofluids [21]. Forced convection achieves a higher heat transfer rate when the concentration of nanoparticles is high, according to studies of the heat transfer process in nanofluids [22].

Nanofluids can be seen in numerous manufacturing sectors, including mechanical engineering and transportation, as well as numerous technologies, including fuel cells, diesel fuel combustion, solar water heating, microdevices, etc. [23]. The flow of a tangent hyperbolic nanofluid in the MHD boundary layer over a stretchable sheet was investigated [24]. Authors investigated how thermal radiation affected the MHD boundary layer flow of a tangent hyperbolic nanofluid with no normal nanoparticle flow over an angled sheet that extended exponentially and had suction [25]. Here, the Runge-Kutta method was used to solve the transformed systems numerically.

Other scholars chose to investigate in depth the influence of variable thermal conductivity and thermal radiation on the MHD tangent hyperbolic fluid in the presence of nanoparticles passing through a stretchable sheet [26]. Heat and mass transfer properties were studied under collective sliding and convection conditions with internal heating, viscous dissipation, and Joule heating. The two-dimensional tangent hyperbolic nanofluid boundary layer equations were obtained.

Previous research investigates the phenomenon of heat and mass transfer resulting from the unsteady MHD flow of Williamson nanofluid in a permeable channel with a heat source/sink [27]. The presented model accounts for the buoyancy and thermal radiation effects. The flow equations are transformed into nonlinear partial differential coupled equations. To obtain solutions to the above nonlinear system, numerical simulations are performed.

Some authors suggested a new way to solve nonlinear boundary value problems, which often arise in similarity problems with a variable boundary layer defined in semi-infinite regions [28]. The proposed method, known as the spectral relaxation method, is based on simple iteration schemes created by decreasing the order of the momentum equation and then rearranging the systems of nonlinear equations that result.

The equations that model the transport processes are typically nonlinear, and they have been solved in numerous papers using various semianalytical or numerical methods. Traditional studies of nanofluids, for example, have used homotopic analysis to solve the equations [29]. Spectral collocation methods, such as spectral local linearisation methods, spectral perturbation, spectral relaxation, sequential linearisation, piecewise sequential linearisation as spectral quasilinearisation, and spectral homotopic analysis methods, have recently been developed. Most boundary value problems have been solved using these methods. Convergence can be achieved quickly and accurately using these methods [30].

Buongiorno developed a nonhomogeneous equilibrium model specifically for nanofluids to facilitate the exploration of mass/heat transfer based on viable theories and assumptions [31]. This innovative model includes slip mechanisms, such as Brownian diffusion and thermophoresis, which occur inside a liquid medium under certain physical constraints.

After the Buongiorno two-phase model was approved, some researchers made further assumptions regarding natural convective flows in a limited nanofluid medium under a negative temperature gradient applied vertically between two horizontal boundaries [32, 33]. In this case, the assumption is that the vertical mass flux of nanoparticles vanishes within these limiting boundaries [32, 33]. In this regard,

other scholars performed a comprehensive numerical analysis of the unsteady convection MHD Couette flows [34]. They estimated the thermal and mass characteristics of copper-based radiative aqueous nanofluids using single-phase and two-phase nanofluid models [34].

To better understand the mechanisms behind thermal enhancement, some researchers analyzed how thermal migration of randomly moving nanoparticles has affected the dynamic and physical characteristics of nanofluidic systems [35, 36]. Even though the two-phase approach is commonly used to model many convection flow issues, scientifically speaking, the assumption of zero nanoparticle flux is still under question. Hence, more studies are needed to investigate the stability of nanofluids.

The first analytical study concerning the stability of electroconvection in a rotating porous medium filled with a dielectric nanofluid was carried out in 2016 [37]. Two years later, researchers found some supporting evidence using several innovative approaches to computation [38]: the Classical Galerkin Weighted Residues Technique (CGWRT), the Power Series Method (PSM), the Polynomial Collocation Method (PCM), the Wakif-Galerkin Weighted Residual Technique (WGWRT), the Chebyshev-Gauss-Lobatto Spectral Method (CGLSM), and the Runge-Kutta-Felberg Method (RKFM). From a methodological perspective, CGWRT fails to correctly take into account thermal stability in a limited nanofluidic medium under the assumption of a zero nanoparticle flux [39]. It gives unacceptable results, for it has a lower level of accuracy than the other methods described above [32, 33].

The Buongiorno model is extended in [40] to investigate the heat transfer and flow characteristics of a three-dimensional (3D) tangent hyperbolic nanofluid. The purpose of this contribution is to investigate the effects of velocity slip and suction on the flow and heat transfer characteristics of a nanofluid. Here, a new boundary condition is implemented under the assumption that the nanoparticle mass flux equals zero.

Considering the preceding publications, this study is aimed at developing a method for studying the dynamics of a three-dimensional tangent hyperbolic flow of a nanofluid over a permeable stretchable sheet using the Buongiorno model. The objectives in this regard are (1) to solve the flow equations using spectral local linearisation, (2) to determine how the local Nusselt number depends on the parameters of Brownian motion of nanoparticles, (3) to determine how velocity profiles depend on the magnetic field parameter and the Prandtl number, and (4) to determine whether temperature and concentration profiles depend on the thermophoresis parameters.

2. Materials and Methods

The study suggests a method for modelling a tangent hyperbolic nanofluid flow over a permeable stretchable sheet in this section (Figure 1).

The present model is based on the following assumptions. (1) The present case considers the Buongiorno nanofluid model. (2) The gravity direction is normal. (3) The flow is affected by a uniform and inclined magnetic field with intensity B. (4) The internal heat release in the flow area is taken at a constant rate. (5) The porous medium is isotropic. (6) Radiation, Joule heating, and viscous dissipation effects can be ignored. (7) The liquid flows through a hydrodynamically and thermally nonhomogeneous porous medium. (8) The permeability and thermal conductivity of a porous medium are nonhomogeneous properties. (9) The porosity is a constant.

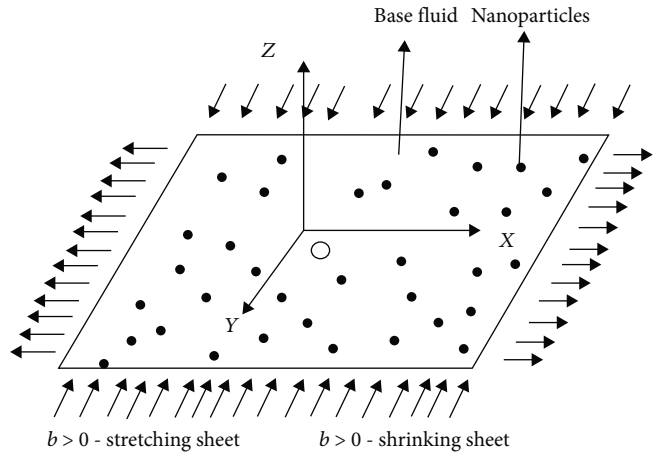

Figure 1: Physical configuration of the proposed model.

The novelty of this article lies in providing evidence that support the following two statements. (1) The Brownian movement of particles has an insignificant effect on the heat transfer rate. (2) The modified Weissenberg number (i.e., the ratio of the elastic force to the viscous force) causes the velocity of the moving fluid to decrease. The study also provides information about the physical influence of different parameters on the nanofluid flow characteristics, the skin friction coefficient, and the local Nusselt number.

This study explores a three-dimensional nanofluid flow using the Buongiorno model. Here, a new boundary condition is implemented with the assumption that the nanoparticle mass flux at the surface is zero. This condition seems practically more realistic because the fraction of nanoparticles at the boundary becomes implicitly controlled. This work investigates the influence of flow and velocity slip on the nanofluid flow and heat transfer characteristics. The basic partial differential equations for momentum, energy, and nanoparticle solid concentration are reduced to ordinary differential equations with the help of appropriate transformations. These equations were then solved with bvp4c in MATLAB.

Here, we consider a stationary three-dimensional incompressible flow of an electrically conducting water-based MHD nanofluid over a convectively heated exponentially stretching sheet. A uniform transverse magnetic field of strength B0 is applied in the z direction. The magnetic Reynolds number is considered small. The induced magnetic and electric fields are ignored. The convective boundary condition is used after the sheet surface gets heated by a hot liquid.

The resulting three-dimensional model has a z coordinate orthogonal to the stretched sheet in the xy plane. The

mass flow velocity w is equal to w_0, whereas in the case of suction,$w_0 > 0$, and in the case of injection,$-w_0 < 0$. The equations for energy, nanoparticle solid concentration, momentum, and mass can be written as

$$\frac{du}{dx} + \frac{dw}{dz} + \frac{dv}{dy} = 0, \tag{1}$$

$$u\frac{du}{dx} + w\frac{du}{dz} + v\frac{du}{dy} = (1-n)v\frac{d^2u}{dz^2} + \sqrt{2}vn\Gamma\frac{du}{dz}\frac{d^2u}{dz^2} - u\frac{B_0^2\sigma}{\rho}, \tag{2}$$

$$u\frac{dv}{dx} + w\frac{dv}{dz} + v\frac{dv}{dy} = (1-n)v\frac{d^2v}{dz^2} + \sqrt{2}vn\Gamma\frac{dv}{dz}\frac{d^2v}{dz^2} - v\frac{B_0^2\sigma}{\rho}, \tag{3}$$

$$u\frac{dc}{dx} + w\frac{dc}{dz} + v\frac{dc}{dy} = \frac{D_T}{T_\infty}\frac{d^2T}{dz^2} + D_B\frac{d^2c}{dz^2}, \tag{4}$$

$$u\frac{dT}{dx} + w\frac{dT}{dz} + v\frac{dT}{dy} = (1-n)v\frac{d^2T}{dz^2} + \beta\left[\frac{D_T}{T_\infty}\left(\frac{dT}{dz}\right)^2 + D_B\frac{dc}{dz}\frac{dT}{dz}\right]. \tag{5}$$

The boundary conditions are as follows [41]:

$$u = u_w(x) = ax + \alpha N_1\frac{du}{dz}, v = v_w(y) = by + \alpha N_2\frac{dv}{dz}, \tag{6}$$

$$T = T_w, w = w_0, \frac{D_T}{T_\infty}\frac{dT}{dz} + D_B\frac{dc}{dz} = 0, z = 0, \tag{7}$$

$$u \longrightarrow 0, v \longrightarrow 0, T \longrightarrow T_\infty, c \longrightarrow c_\infty, z \longrightarrow \infty, \tag{8}$$

where C is the nanoparticle volume; T_w is the constant surface temperature; T is the temperature of the nanofluid; C_∞ and T_∞ are the nanoparticle volume and the temperature of the surrounding fluid, respectively; v is the kinematic viscosity of the nanofluid; α is the thermal conductivity of the nanofluid; N_1 and N_2 are constant slip coefficients; n is the power index; D_B is the Brownian diffusion coefficient; D_T is the thermophoretic diffusion coefficient; σ is the electrical conductivity of the fluid; Γ is the Williamson parameter; p is the nanofluid density; B_0 is the magnetic induction parameter; and u, v, and w are the velocity components along the directions $x - y - z$, respectively.

$$\beta = \frac{C_p}{C_f}, \tag{9}$$

where C_f is the heat capacitance of the nanofluid and C_p is the heat capacitance of the solid nanoparticle.

Further, we have the following assumption: $v_w(y) = yb$ and $u_w(x) = xa$, with constants $a > 0$ and $b < 0$, which correspond to a shrinking sheet, and $a > 0$ and $b > 0$, which correspond to a stretching sheet.

Due to Brownian motion $(D_T/T_\infty)(dT/dz) + dc/dz = 0$ (if $z = 0$) and the boundary condition D_B, the fraction of nanoparticles is controlled passively rather than actively. This condition ensures that nanoparticles move chaotically at the boundary.

The similarity transformations are as follows [42]:

$$v = yag'(\eta), u = xaf'(\eta), w = -\sqrt{\alpha a}[f(\eta) + g(\eta)], \tag{10}$$

$\varphi(\eta) = C - C_\infty/C_\infty, \theta(\eta) = T - T_\infty/T_w - T_\infty, \eta = \sqrt{a/\alpha}z$, where f and g denote the dimensionless flow function and the dashes denote differentiation by n.

Given (10), equations (2)–(6) will be expressed as

$$\mathrm{Pr}f''\left((1-n) + n\mathrm{We}_x f''\right) + f''(f+g) - f'^2 - Mf' = 0, \tag{11}$$

$$\mathrm{Pr}g''\left((1-n) + n\mathrm{We}_y g''\right) + g''(f+g) - g'^2 - Mg' = 0, \tag{12}$$

$$\theta'(f+g) + \theta'' + \mathrm{Nt}\theta'^2 + \mathrm{Nb}\theta'\varphi' = 0, \tag{13}$$

$$\mathrm{Le}\varphi'(f+g) + \varphi'' + \frac{\mathrm{Nt}}{\mathrm{Nb}}\theta'' = 0. \tag{14}$$

The dimensionless boundary conditions will be as follows:

$$g'(0) = Bg''(0) + \lambda, f'(0) = Af''(0) + 1, g(0) = 0, \tag{15}$$

$$f(0) = S, \theta(0) = 1, \varphi'(0) + (\mathrm{Nt}/\mathrm{Nb})\theta'(0) = 0,$$
$$g'(\infty) = 0, f'(\infty) = 0, \varphi(\infty) = 0, \theta(\infty) = 0,$$

where M is the magnetic field parameter, A and B are dimensionless sliding parameters, We_y and We_x are Weissenberg numbers, and λ is the constant stretching parameter, while $\lambda < 0$ indicates a shrinking sheet, and $\lambda > 0$ means a stretching sheet.

The constant mass flow S is one of the most crucial parameters in this study. While $S < 0$ represents injection, $S > 0$ represents suction, and $S = 0$ represents an impermeable plate; Le is the Lewis number; Nt and Nb are thermophoresis and Brownian motion parameters, respectively; and Pr is the Prandtl number.

These parameters are set as follows:

$$\mathrm{We}_y = \sqrt{\frac{a}{\alpha}}ya\sqrt{2\Gamma}, \mathrm{We}_x = \sqrt{\frac{a}{\alpha}}xa\sqrt{2\Gamma},$$
$$M = \frac{B_0^2\sigma}{a\rho}, \lambda = \frac{b}{a}, \mathrm{Pr} = \frac{\nu}{\alpha},$$
$$S = -\frac{w_0}{\sqrt{\alpha a}}, \mathrm{Le} = \frac{\alpha}{D_B}, A = N_1\sqrt{\alpha a}, B = N_2\sqrt{\alpha a}. \tag{16}$$

The local coefficients of surface friction Cf_y and Cf_x, as well as the local Nusselt number Nu_x, are set as follows:

$$\mathrm{Cf}_x = \frac{\tau_{xw}}{U_w^2\rho}, \mathrm{Cf}_y = \frac{\tau_{yw}}{V_w^2\rho}, \mathrm{Nu}_x = \frac{q_w x}{(T_w - T_\infty)k}, \tag{17}$$

where τ_{yw} and τ_{xw} are coefficients of surface friction in the y and x directions and q_w is the heat flux from the sheet surface.

The above coefficients are found as follows:

$$\begin{aligned}
\tau_{yw} &= \mu\left((1-n)\frac{dv}{dz} + \frac{\Gamma n}{\sqrt{2}}\left(\frac{dv}{dz}\right)^2\right)\Bigg|_{z=0},\\
\tau_{xw} &= \mu\left((1-n)\frac{du}{dz} + \frac{\Gamma n}{\sqrt{2}}\left(\frac{du}{dz}\right)^2\right)\Bigg|_{z=0},\\
q_w &= -k\left(\frac{dT}{dz}\right)\Bigg|_{z=0}.
\end{aligned} \tag{18}$$

3. Results

By using equation (17), and then substituting equation (12) into equation (18), one arrives at the following equation:

$$\begin{aligned}
\lambda^{1,5}\mathrm{Cf}_y\left(\frac{\mathrm{Re}_x}{\mathrm{Pr}}\right)^{0,5} &= (1-n)g''(0) + \frac{\mathrm{We}_y n}{2}g''(0)^2,\\
\mathrm{Cf}_x\left(\frac{\mathrm{Re}_x}{\mathrm{Pr}}\right)^{0,5} &= (1-n)f''(0) + \frac{\mathrm{We}_x n}{2}f''(0)^2,\\
\mathrm{Nu}_x &= -\theta'(0),
\end{aligned} \tag{19}$$

where $\mathrm{Re}_x = xu_w/v$ and $\mathrm{Re}_y = yu_w/v$ are Reynolds numbers.

The author of this article uses spectral local linearisation to solve the nonlinear boundary value problem defined by equations (11)–(14) with boundary conditions (15). The Gauss-Seidel method and the Bellman and Kalaba quasilinearisation method [43] are combined in this solution for equation separation.

The spectral local linearisation method linearises the nonlinear components and decouples the system of equations. Furthermore, the Chebyshev spectral collocation method is used to approximate the solution of the linearised system. Scientists, for example, in studies [44, 45], used this method to solve mathematical models. For example, [46] gives a description of this method for differential equation systems.

Spectral local linearisation applied to equations (11)–(14) yields the following dependencies:

$$f'''_{r+1}a_{0,r} + f''_{r+1}a_{1,r} + f'_{r+1}a_{2,r} + f_{r+1}a_{3,r} = R_{1,r}, \tag{20}$$

$$f''_{r+1}b_{0,r} + f'_{r+1}b_{1,r} + f'_{r+1}b_{2,r} + f_{r+1}b_{3,r} = R_{2,r}, \tag{21}$$

$$\theta'_{r+1}c_{1,r} + \theta'_{r+1} = R_{3,r}, \tag{22}$$

$$\varphi'_{r+1}d_{1,r} + \varphi''_{r+1} = R_{4,r}, \tag{23}$$

where dashes denote partial derivatives with respect to n. Here, the boundary conditions are set by the expressions

$$f_{r+1}(0) = S, f'_{r+1}(\infty) = 0, f'_{r+1}(0) = Af'_{r+1}(0) + 1, \tag{24}$$

$$\begin{aligned}
&g_{r+1}(0) = 0, g'_{r+1}(\infty) = 0, g'_{r+1}(0) = Bg'_{r+1}(0) + \lambda,\\
&\theta'_{r+1}(\infty) = 0, \theta_{r+1}(0) = 1,\\
&\varphi_{r+1}(\infty) = 0, \varphi'_{r+1}(0) + (\mathrm{Nt}/\mathrm{Nb})\theta'_r(0) = 0.
\end{aligned}$$

In equations (20)–(23), the coefficients can be found as follows:

$$a_{0,r} = \left(\mathrm{We}_x n f'' - n + 1\right)\mathrm{Pr}, a_{1,r} = \mathrm{We}_x n\mathrm{Pr}f'''_r + f_r + g_r, \tag{25}$$

$$a_{2,r} = -(2f'_r + M), a_{3,r} = f''_r,$$

$$b_{0,r} = \left(\mathrm{We}_x n g'' - n + 1\right)\mathrm{Pr}, b_{1,r} = \mathrm{We}_x n\mathrm{Pr}g'''_r + f_r + g_r, \tag{26}$$

$$b_{2,r} = -(2g'_r + M), b_{3,r} = g''_r,$$

$$\begin{aligned}
c_{1,r} &= bN\varphi' + 2tN\theta' + f_r + g_r,\\
d_{1,r} &= eL(g_r + f_r),\\
R_{1,r} &= f'''_r a_{0,r} + f''_r a_{1,r} + f'_r a_{2,r} + f_r a_{3,r} - F_1,\\
R_{2,r} &= g'''_r b_{0,r} + g''_r b_{1,r} + g'_r b_{2,r} + g_r b_{3,r} - F_2,\\
R_{3,r} &= \theta''_r + \theta'_r c_{1,r} - F_3,\\
R_{4,r} &= \varphi''_r + \varphi'_r d_{1,r} - F_4.
\end{aligned} \tag{27}$$

The region $\eta \in [0, L_\infty]$ can be transformed into the interval $x \in [-1, 1]$ using a suitable linear transformation. The author defines the Gauss-Lobatto grid points as follows:

$$x_j = \cos\frac{j\pi}{N_3}, \quad j = 0, 1, \cdots, N. \tag{28}$$

Unknown functions are represented as matrices. Their Chebyshev differentiation matrix derivatives are as follows:

$$\frac{df}{dx} = \sum_{k=0}^{N} D_{jk}f(x_k) = DF, \quad j = 0, 1, \cdots, N. \tag{29}$$

In this respect, the higher-order derivatives are written as follows:

$$\frac{d^n f}{dx^n} = D^n F, \tag{30}$$

where D is the differentiation by n and n is the order of the derivative.

In this respect,

$$F = [f(x_0), f(x_1), \cdots, f(x_N)]^T. \tag{31}$$

Then, in equations (20)–(23), the spectral method is used to derive the following equation:

$$\begin{aligned} R_{1,r} &= \left(D^3 a_{0,r} + D^2 a_{1,r} + D a_{2,r} + I a_{3,r}\right) F_{r+1}, \\ R_{2,r} &= \left(D^3 b_{0,r} + D^2 b_{1,r} + D b_{2,r} + I b_{3,r}\right) G_{r+1}, \\ R_{3,r} &= \left(D^2 + D c_{1,r}\right) \theta_{r+1}, \\ R_{4,r} &= \left(D^2 + D d_{1,r}\right) \varphi_{r+1}, \end{aligned} \tag{32}$$

where I is a unit matrix $(N+1)\times(N+1)$ and the coefficients in bold are diagonal matrices. The matrix will be written as

$$R_{1,r} = AF_{r+1}, R_{2,r} = BG_{r+1}, R_{3,r} = C\theta_{r+1}, R_{4,r} = E\phi_{r+1}. \tag{33}$$

In this respect,

$$\begin{aligned} A &= D^3 a_{0,r} + D^2 a_{1,r} + D a_{2,r} + I a_{3,r}, \\ B &= D^3 b_{0,r} + D^2 b_{1,r} + D b_{2,r} + I b_{3,r}, \\ C &= D_2 + D c_{1,r}, E = D_2 + D d_{1,r}. \end{aligned} \tag{34}$$

Then, by iteratively solving equation (33), starting with suitable initial solutions, approximate solutions for θ, ϕ, f, and g are derived.

The conservation equations are then solved by spectral local linearisation [47]. Figures 2–9 show the dependencies of the numerical simulation results.

4. Discussion

The author verified the accuracy of the obtained results by comparing the solutions they presented with the results published in [48] for a variety of parameter values.

Figure 2 shows how the magnetic field parameters M affect the concentration $\phi(\eta)$ and temperature $\theta(\eta)$ profiles. The research results indicate that the concentration and temperature profiles increase with increasing magnetic field parameters, as shown in the figure. The research [49] supports this conclusion. This is because an increase in electromagnetic forces causes fluid movement to slow down. The concentration and temperature boundary layers subsequently thicken, according to the researchers who wrote this article.

Figure 3 shows how the magnetic parameter M changes based on velocity profiles. It is important to note here that the velocities as $g'(n)$ and $f'(n)$ decrease with increasing magnetic field parameters. This is explained by electromagnetic interactions between magnetic fields and electrically conductive nanofluids. This interaction produces the slowing Lorentz force, which reduces the velocity of fluids in the boundary layers, and this phenomenon is well supported by data [50]. Consequently, the magnetic field parameter presence has a substantial effect on flow dynamics. Additionally, it can be deduced that $g'(n)$ has lower values than $f'(\eta)$ for various fixed values of M.

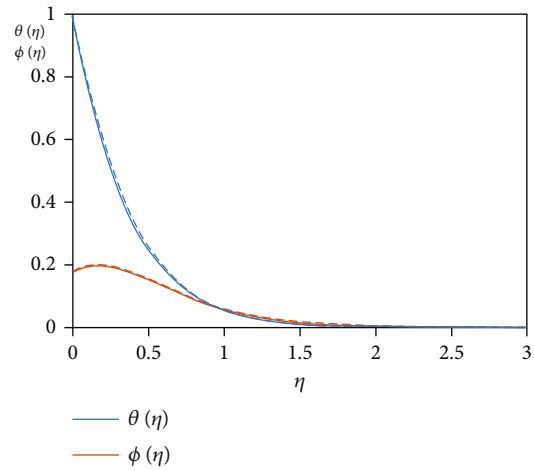

Figure 2: Concentration and temperature profiles affected by magnetic field parameters.

Figures 4 and 5 show how the change in the Weissenberg number depends on the temperature, velocity, and concentration of nanoparticles. Here, an increase in the Weissenberg number (Figure 4) leads to the increase in the temperature and concentration profiles. This finding is consistent with previous research [51]. Increases in the Weissenberg number parallel to the axes, on the other hand, cause a decrease in velocities. This makes sense, since the Weissenberg numbers show the relationship between the shear rate and the relaxation time. Hence, as the Weissenberg numbers increase, so does the relaxation time. Therefore, higher resistances arise, and consequently, the velocity profiles decrease. Figure 5 shows one example of this.

Figure 6 shows what happens to the nanoparticle concentration and temperature profiles when the Prandtl number changes. As can be seen, as the Prandtl numbers rise, the profiles of temperature and nanoparticle concentration at a particular point decrease, which is supported by the authors in [52]. Physically speaking, the cause could be that a rise in Prandtl numbers causes a fall in thermal conductivity, which in turn causes a fall in the concentration and thermal thickness of boundary layers.

Figure 7 shows how the Prandtl number affects velocity profiles with fixed parameters. It is not difficult to conclude that as the Prandtl number increases, the velocity profiles increase close to the boundary layers, and this is supported by the study [53]. It can further be argued that for any fixed values of the Prandtl number Pr and η, $g'(\eta)$ has lower values than $f'(\eta)$.

Figure 8 shows how the thermophoresis parameters change based on the concentration and temperature profiles. It is plain to see that as the values of Nt increase, the concentration and temperature profiles increase as they approach the boundary. This is reflected in the robot's results as well [54–57]. Furthermore, for any fixed value of n, anything near the boundary$\phi(n)$ will assume a smaller value than $\theta($ $\eta)$. Another notable point is the sharp increase in concentration profiles near the boundary as Nt increases. The reason for the temperature profile $\theta(n)$ increasing could be that as

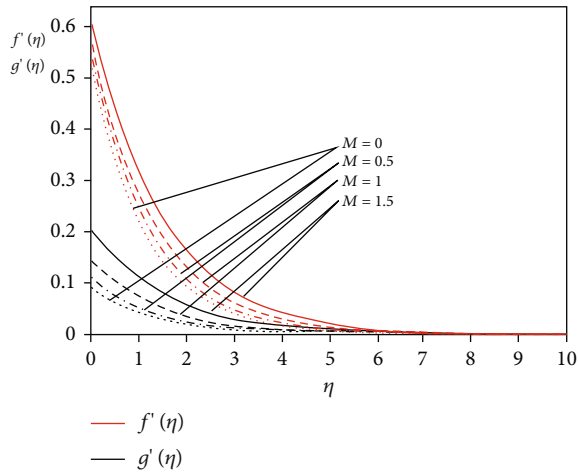

Figure 3: Velocity profiles affected by magnetic field parameters.

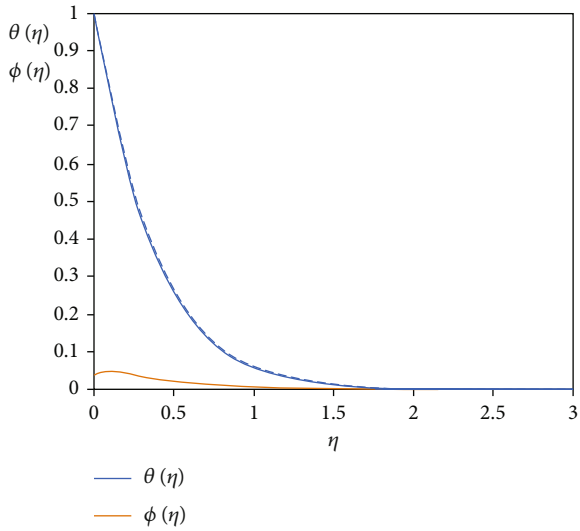

Figure 4: Concentration and temperature profiles affected by the Weissenberg number.

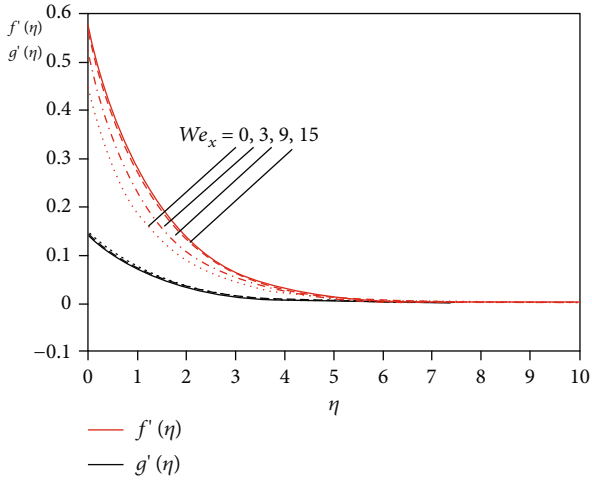

Figure 5: Velocity profiles affected by the Weissenberg number.

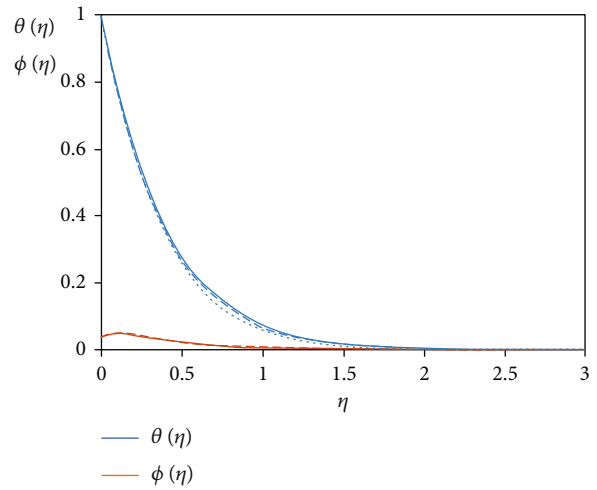

Figure 6: Concentration and temperature profiles affected by the Prandtl numbers.

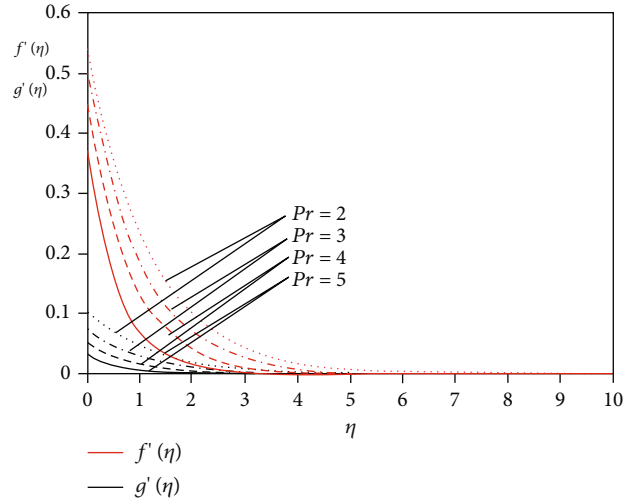

Figure 7: Velocity profiles affected by the Prandtl number.

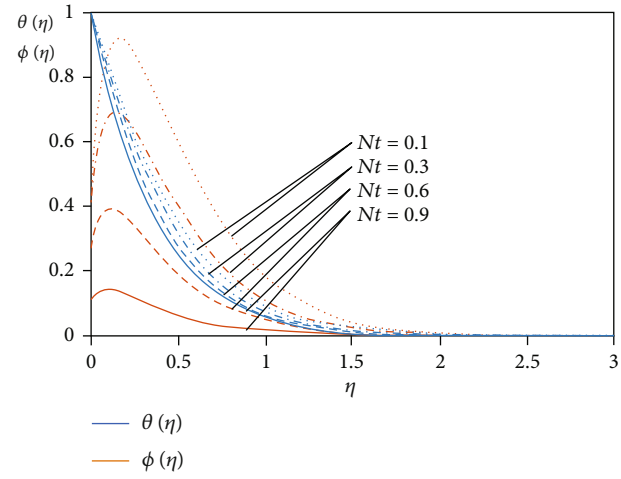

Figure 8: Concentration and temperature profiles affected by thermophoresis parameters.

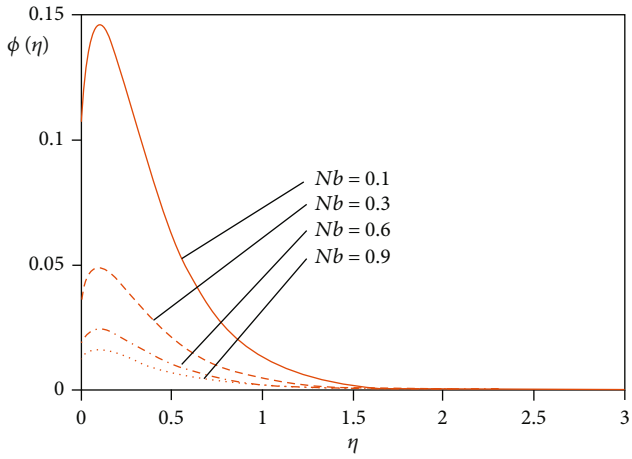

Figure 9: Concentration profiles affected by Brownian motion parameters.

Nt increases, so does the transfer of fluid to the cold region from the hot one, causing the fluid temperature to rise.

Figure 9 shows how the parameters of Brownian motion affect the concentration profiles. It has been discovered that as the Brownian motion of nanoparticles increases, so do their concentration profiles. This can be explained by the fact that as the Brownian motion of nanoparticles increases, more intense mixing and uneven movement of the nanofluid begins to occur, leading to a decrease in the nanoparticle concentration profiles.

5. Conclusions

This study uses the Buongiorno model and a permeable, stretchable sheet to study the dynamics of three-dimensional tangent hyperbolic nanofluid flows. The assumption was that the flux fields were subjected to magnetic field effects, which impacted the change in nanofluid flows.

Using spectral local linearisation, the flow equations can be solved successfully. The proposed method has been shown to produce highly precise results.

When the Brownian motion parameters change, the Nusselt number does not change significantly. This suggests that the Brownian motion of nanoparticles is restricted, which has a significant impact on the thermal conductivity of nanofluids.

The Nusselt number decreases with increasing thermophoresis parameters. Nanoparticle diffusion into cold zones increases with increasing thermophoresis, which explains this phenomenon physically. This, in turn, increases the thickness of the thermal boundary layers, which further contributes to a reduction in the rates at which heat is transferred.

It has been established that changes in the Nusselt number at fixed values of thermophoresis parameters do not occur as Brownian motion parameters increase. Alongside this, the Nusselt number decreases as the thermophoretic parameter increases for a fixed parameter of Brownian motion.

When the thermophoresis parameters are changed, the concentration profiles increase significantly near the boundaries.

When the values of the magnetic field parameters are increased while all the other parameters remain unchanged, there is a corresponding decrease in the velocity profiles at points that are close to the boundaries.

The velocity profiles increase as Prandtl numbers increase while other model parameters stay constant.

As the thermophoresis parameters increase, so do the concentration and temperature profiles.

Data Availability

Data will be available on request.

Conflicts of Interest

The author declared no potential conflicts of interest with respect to the research, authorship, and/or publication of this article.

Acknowledgments

Dayong Nie was supported by the Young Key Teachers Project in Higher Vocational Colleges of Henan Province (Grant Number: 2020GZGG109) and Key Research Projects in Colleges of Henan Province (Grant Number: 23B110016).

References

[1] X. Su, L. Zheng, X. Zhang, and J. Zhang, "MHD mixed convective heat transfer over a permeable stretching wedge with thermal radiation and ohmic heating," *Chemical Engineering Science*, vol. 78, pp. 1–8, 2012.

[2] M. H. Esfe and M. R. Sarlak, "Experimental investigation of switchable behavior of CuO-MWCNT (85%–15%)/10W-40 hybrid nano-lubricants for applications in internal combustion engines," *Journal of Molecular Liquids*, vol. 242, pp. 326–335, 2017.

[3] M. Hamid, T. Zubair, M. Usman, Z. H. Khan, and W. Wang, "Natural convection effects on heat and mass transfer of slip flow of time-dependent Prandtl fluid," *Journal of Computational Design and Engineering*, vol. 6, no. 4, pp. 584–592, 2019.

[4] M. A. Qureshi, "A case study of MHD driven Prandtl-Eyring hybrid nanofluid flow over a stretching sheet with thermal jump conditions," *Case Studies in Thermal Engineering*, vol. 28, article 101581, 2021.

[5] E. Hosseini, G. B. Loghmani, M. Heydari, and M. M. Rashidi, "Numerical investigation of velocity slip and temperature jump effects on unsteady flow over a stretching permeable surface," *The European Physical Journal Plus*, vol. 132, no. 2, article 96, 2017.

[6] S. Ghosh, S. Mukhopadhyay, and K. Vajravelu, "Dual solutions of slip flow past a nonlinearly shrinking permeable sheet," *Alexandria Engineering Journal*, vol. 55, no. 2, pp. 1835–1840, 2016.

[7] M. Waqas, M. Farooq, M. I. Khan, A. Alsaedi, T. Hayat, and T. Yasmeen, "Magnetohydrodynamic (MHD) mixed convection flow of micropolar liquid due to nonlinear stretched sheet

with convective condition," *International Journal of Heat and Mass Transfer*, vol. 102, pp. 766–772, 2016.

[8] S. Zeb, S. Khan, Z. Ullah et al., "Lie group analysis of double diffusive MHD tangent hyperbolic fluid flow over a stretching sheet," *Mathematical Problems in Engineering*, vol. 2022, Article ID 9919073, 14 pages, 2022.

[9] A. Hussain, A. Hassan, Q. Al Mdallal et al., "Heat transport investigation of magneto-hydrodynamics (SWCNT-MWCNT) hybrid nanofluid under the thermal radiation regime," *Case Studies in Thermal Engineering*, vol. 27, article 101244, 2021.

[10] T. Hayat, M. Waqas, S. A. Shehzad, and A. Alsaedi, "MHD stagnation point flow of Jeffrey fluid by a radially stretching surface with viscous dissipation and Joule heating," *Journal of Hydrology and Hydromechanics*, vol. 63, no. 4, pp. 311–317, 2015.

[11] O. D. Makinde, F. Mabood, W. A. Khan, and M. S. Tshehla, "MHD flow of a variable viscosity nanofluid over a radially stretching convective surface with radiative heat," *Journal of Molecular Liquids*, vol. 219, pp. 624–630, 2016.

[12] M. Waqas, M. I. Khan, T. Hayat, M. M. Gulzar, and A. Alsaedi, "Transportation of radiative energy in viscoelastic nanofluid considering buoyancy forces and convective conditions," *Chaos, Solitons & Fractals*, vol. 130, article 109415, 2020.

[13] A. G. N. Sofiah, M. Samykano, A. K. Pandey, K. Kadirgama, K. Sharma, and R. Saidur, "Immense impact from small particles: review on stability and thermophysical properties of nanofluids," *Sustainable Energy Technologies and Assessments*, vol. 48, article 101635, 2021.

[14] W. T. Urmi, M. M. Rahman, K. Kadirgama, D. Ramasamy, and M. A. Maleque, "An overview on synthesis, stability, opportunities and challenges of nanofluids," *Materials Today: Proceedings*, vol. 41, pp. 30–37, 2021.

[15] T. Islam, M. Yavuz, N. Parveen, and M. Fayz-Al-Asad, "Impact of non-uniform periodic magnetic field on unsteady natural convection flow of nanofluids in square enclosure," *Fractal and Fractional*, vol. 6, no. 2, p. 101, 2022.

[16] M. Shoaib, G. Zubair, M. A. Z. Raja, K. S. Nisar, A.-H. Abdel-Aty, and I. S. Yahia, "Study of 3-D Prandtl nanofluid flow over a convectively heated sheet: a stochastic intelligent technique," *Coatings*, vol. 12, no. 1, p. 24, 2022.

[17] A. S. Dogonchi, M. Waqas, S. R. Afshar et al., "Investigation of magneto-hydrodynamic fluid squeezed between two parallel disks by considering Joule heating, thermal radiation, and adding different nanoparticles," *International Journal of Numerical Methods for Heat & Fluid Flow*, vol. 30, no. 2, pp. 659–680, 2020.

[18] S. Choi and J. A. Estman, "Enhancing thermal conductivity of fluids with nanoparticles," in *ASME International Mechanical Engineering Congress & Exposition*, vol. 231, pp. 99–106, San Francisco, CA, 1995.

[19] C. Liu, Y. Qiao, P. Du et al., "Recent advances of nanofluids in micro/nano scale energy transportation," *Renewable and Sustainable Energy Reviews*, vol. 149, article 111346, 2021.

[20] M. K. Mishra, G. S. Seth, and R. Sharma, "Navier's slip effect on mixed convection flow of non-Newtonian nanofluid: Buongiorno's model with passive control approach," *International Journal of Applied and Computational Mathematics*, vol. 5, no. 4, pp. 1–23, 2019.

[21] A. S. Dogonchi, M. Hashemi-Tilehnoee, M. Waqas, S. M. Seyyedi, I. L. Animasaun, and D. D. Ganji, "The influence of different shapes of nanoparticles on Cu-H_2O nanofluids in a partially heated irregular wavy enclosure," *Physica A: Statistical Mechanics and its Applications*, vol. 540, article 123034, 2020.

[22] R. Saidur, K. Y. Leong, and H. A. Mohammad, "A review on applications and challenges of nanofluids," *Renewable and Sustainable Energy Reviews*, vol. 15, no. 3, pp. 1646–1668, 2011.

[23] J. Fan and L. Wang, "Review of heat conduction in nanofluids," *Journal of Heat Transfer*, vol. 133, no. 4, article 040801, 2011.

[24] M. Waqas, G. Bashir, T. Hayat, and A. Alsaedi, "On non-Fourier flux in nonlinear stretching flow of hyperbolic tangent material," *Neural Computing and Applications*, vol. 31, no. S1, pp. 597–605, 2019.

[25] N. Saidulu, T. Gangaiah, and A. V. Lakshmi, "Radiation effect on MHD flow of a tangent hyperbolic nanofluid over an inclined exponentially stretching sheet," *International Journal of Fluid Mechanics Research*, vol. 46, no. 3, pp. 277–293, 2019.

[26] S. M. Atif, S. Hussain, and M. Sagheer, "Effect of viscous dissipation and Joule heating on MHD radiative tangent hyperbolic nanofluid with convective and slip conditions," *Journal of the Brazilian Society of Mechanical Sciences and Engineering*, vol. 41, no. 4, article 189, 2019.

[27] M. Hamid, M. Usman, Z. H. Khan, R. U. Haq, and W. Wang, "Numerical study of unsteady MHD flow of Williamson nanofluid in a permeable channel with heat source/sink and thermal radiation," *The European Physical Journal Plus*, vol. 133, no. 12, article 527, 2018.

[28] S. S. Motsa, "A new spectral relaxation method for similarity variable nonlinear boundary layer flow systems," *Chemical Engineering Communications*, vol. 201, no. 2, pp. 241–256, 2014.

[29] T. M. Agbaje, S. Mondal, Z. G. Makukula, S. S. Motsa, and P. Sibanda, "A new numerical approach to MHD stagnation point flow and heat transfer towards a stretching sheet," *Ain Shams Engineering Journal*, vol. 9, no. 2, pp. 233–243, 2018.

[30] I. S. Oyelakin, S. Mondal, and P. Sibanda, "Unsteady Casson nanofluid flow over a stretching sheet with thermal radiation, convective and slip boundary conditions," *Alexandria Engineering Journal*, vol. 55, no. 2, pp. 1025–1035, 2016.

[31] J. Buongiorno, "Convective transport in nanofluids," *Journal of Heat Transfer*, vol. 128, no. 3, pp. 240–250, 2006.

[32] D. A. Nield and A. V. Kuznetsov, "The onset of convection in a horizontal nanofluid layer of finite depth: a revised model," *International Journal of Heat and Mass Transfer*, vol. 77, pp. 915–918, 2014.

[33] G. Rasool, N. A. Ahammad, M. R. Ali et al., "Hydrothermal and mass aspects of MHD non-Darcian convective flows of radiating thixotropic nanofluids nearby a horizontal stretchable surface: passive control strategy," *Case Studies in Thermal Engineering*, vol. 42, article 102654, 2023.

[34] A. Wakif, Z. Boulahia, F. Ali, M. R. Eid, and R. Sehaqui, "Numerical analysis of the unsteady natural convection MHD Couette nanofluid flow in the presence of thermal radiation using single and two-phase nanofluid models for Cu–water nanofluids," *International Journal of Applied and Computational Mathematics*, vol. 4, no. 3, p. 81, 2018.

[35] I. L. Animasaun, R. O. Ibraheem, B. Mahanthesh, and H. A. Babatunde, "A meta-analysis on the effects of haphazard motion of tiny/nano-sized particles on the dynamics and other

physical properties of some fluids," *Chinese Journal of Physics*, vol. 60, pp. 676–687, 2019.

[36] A. Wakif, I. L. Animasaun, P. V. Satya Narayana, and G. Sarojamma, "Meta-analysis on thermo-migration of tiny/nano-sized particles in the motion of various fluids," *Chinese Journal of Physics*, vol. 68, pp. 293–307, 2020.

[37] B. B. Divya, G. Manjunatha, C. Rajashekhar, H. Vaidya, and K. V. Prasad, "Effects of inclined magnetic field and porous medium on peristaltic flow of a Bingham fluid with heat transfer," *Journal of Applied and Computational Mechanics*, vol. 7, no. 4, pp. 1892–1906, 2021.

[38] A. Wakif, Z. Boulahia, and R. Sehaqui, "A semi-analytical analysis of electro-thermo-hydrodynamic stability in dielectric nanofluids using Buongiorno's mathematical model together with more realistic boundary conditions," *Results Physics*, vol. 9, pp. 1438–1454, 2018.

[39] A. K. Rostami, K. Hosseinzadeh, and D. D. Ganji, "Hydrothermal analysis of ethylene glycol nanofluid in a porous enclosure with complex snowflake shaped inner wall," *Waves in Random and Complex Media*, vol. 32, no. 1, pp. 1–18, 2022.

[40] R. Jusoh, R. Nazar, and I. Pop, "Three-dimensional flow of a nanofluid over a permeable stretching/shrinking surface with velocity slip: a revised model," *Physics of Fluids*, vol. 30, no. 3, article 033604, 2018.

[41] T. E. Priya and S. P. A. Devi, "Buongiorno model with revised boundary conditions for hydromagnetic forced convective nanofluid flow past a rotating porous disk," *International Journal of Mathematics Trends and Technology*, vol. 55, no. 3, pp. 212–222, 2018.

[42] S. Khatun and R. Nasrin, "Numerical modeling of Buongiorno's nanofluid on free convection: thermophoresis and Brownian effects," *Journal of Naval Architecture and Marine Engineering*, vol. 18, no. 2, pp. 217–239, 2021.

[43] H. Sithole, H. Mondal, and P. Sibanda, "Entropy generation in a second grade magnetohydrodynamic nanofluid flow over a convectively heated stretching sheet with nonlinear thermal radiation and viscous dissipation," *Results Physics*, vol. 9, pp. 1077–1085, 2018.

[44] H. M. Sithole, S. Mondal, P. Sibanda, and S. S. Motsa, "An unsteady MHD Maxwell nanofluid flow with convective boundary conditions using spectral local linearization method," *Open Physics*, vol. 15, no. 1, pp. 637–646, 2017.

[45] S. Motsa and I. Animasaun, "A new numerical investigation of some thermo-physical properties on unsteady MHD non-Darcian flow past an impulsively started vertical surface," *Thermal Science*, vol. 19, Supplement 1, pp. 249–258, 2015.

[46] S. S. Motsa, Z. G. Makukula, and S. Shateyi, "Spectral local linearisation approach for natural convection boundary layer flow," *Mathematical Problems in Engineering*, vol. 2013, Article ID 765013, 7 pages, 2013.

[47] N. S. Akbar, S. Nadeem, R. U. Haq, and Z. H. Khan, "Numerical solutions of magnetohydrodynamic boundary layer flow of tangent hyperbolic fluid towards a stretching sheet," *Indian Journal of Physics*, vol. 87, no. 11, pp. 1121–1124, 2013.

[48] O. Mahian, L. Kolsi, M. Amani et al., "Recent advances in modeling and simulation of nanofluid flows-part I: fundamentals and theory," *Physics Reports*, vol. 790, pp. 1–48, 2019.

[49] N. Abbas, S. Nadeem, A. Saleem, M. Y. Malik, A. Issakhov, and F. M. Alharbi, "Models base study of inclined MHD of hybrid nanofluid flow over nonlinear stretching cylinder," *Chinese Journal of Physics*, vol. 69, pp. 109–117, 2021.

[50] A. Wakif, A. Chamkha, T. Thumma, I. L. Animasaun, and R. Sehaqui, "Thermal radiation and surface roughness effects on the thermo-magneto-hydrodynamic stability of alumina–copper oxide hybrid nanofluids utilizing the generalized Buongiorno's nanofluid model," *Journal of Thermal Analysis and Calorimetry*, vol. 143, no. 2, pp. 1201–1220, 2021.

[51] A. Wakif and R. Sehaqui, "Generalized differential quadrature scrutinization of an advanced MHD stability problem concerned water-based nanofluids with metal/metal oxide nanomaterials: a proper application of the revised two-phase nanofluid model with convective heating and through-flow boundary conditions," *Numerical Methods for Partial Differential Equations*, vol. 38, no. 3, pp. 608–635, 2020.

[52] R. J. P. Gowda, R. N. Kumar, B. C. Prasannakumara, B. Nagaraja, and B. J. Gireesha, "Exploring magnetic dipole contribution on ferromagnetic nanofluid flow over a stretching sheet: an application of Stefan blowing," *Journal of Molecular Liquids*, vol. 335, article 116215, 2021.

[53] L. Yang, W. Ji, M. Mao, and J.-n. Huang, "An updated review on the properties, fabrication and application of hybrid-nanofluids along with their environmental effects," *Journal of Cleaner Production*, vol. 257, article 120408, 2020.

[54] W. Jamshed, M. R. Eid, K. S. Nisar et al., "A numerical frame work of magnetically driven Powell-Eyring nanofluid using single phase model," *Scientific Reports*, vol. 11, no. 1, article 16500, 2021.

[55] A. Mukhametov, N. Bekhorashvili, A. Avdeenko, and A. Mikhaylov, "The impact of growing legume plants under conditions of biologization and soil cultivation on chernozem fertility and productivity of rotation crops," *Legume Research - An International Journal*, vol. 44, no. 10, pp. 1219–1225, 2021.

[56] A. Mukhametov, D. Snegirev, and I. Petunina, "Selecting an indicator system to assess the adequacy level of agricultural technologies," *International Review of Mechanical Engineering (IREME)*, vol. 15, no. 4, pp. 209–218, 2021.

[57] A. E. Mukhametov, D. R. Dautkanova, and G. N. Zhakupova, "Oxidation of vegetable fats and methods of their analysis," *Journal of Engineering and Applied Science*, vol. 13, Supplement 8, pp. 6462–6466, 2018.